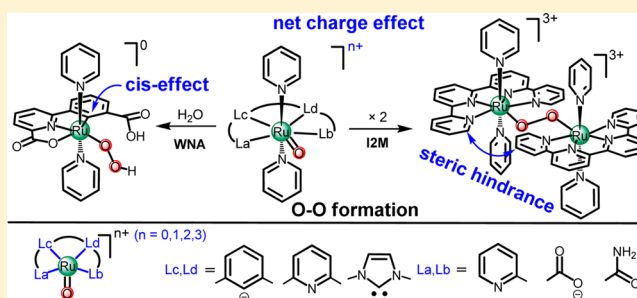


## Probing Ligand Effects on O–O Bond Formation of Ru-Catalyzed Water Oxidation: A Computational Survey

Runhua Kang,<sup>†</sup> Kejuan Chen,<sup>†</sup> Jiannian Yao,<sup>\*,†</sup> Sason Shaik,<sup>‡</sup> and Hui Chen<sup>\*,†</sup><sup>†</sup>Beijing National Laboratory for Molecular Sciences (BNLMS), CAS Key Laboratory of Photochemistry, Institute of Chemistry, Chinese Academy of Sciences, Beijing, 100190, China<sup>‡</sup>Institute of Chemistry and the Lise Meitner-Minerva Center for Computational Quantum Chemistry, The Hebrew University of Jerusalem, Givat Ram Campus, 91904, Jerusalem, Israel

## Supporting Information

**ABSTRACT:** Ligand effects of some representative monomeric Ru-based water oxidation catalysts on the key O–O formation step are revealed in this work. Three effects, namely, cis-effect, net charge effect, and steric hindrance effect, are identified, which can exert sizable modulation on the O–O formation barriers for the two widely accepted O–O formation mechanisms of WNA (water nucleophilic attack) and I2M (direct coupling of two high-valent metal oxo units). The study demonstrates that, through the way of ligand design, there remains a large space for improving O–O bond formation reactivity.



## INTRODUCTION

Searching for highly efficient catalysts for water oxidation ( $2\text{H}_2\text{O} \rightarrow 4\text{H}^+ + 4\text{e}^- + \text{O}_2$ ) has become an important objective in artificial photosynthesis as means for solar energy conversion into a fuel.<sup>1–7</sup> In nature, water oxidation transpires by the  $\text{Mn}_4\text{CaO}_5$  cluster at the oxygen-evolving center (OEC) of photosystem II with a perfect efficiency and high rate that synthetic catalysts have seldom approached to this day.<sup>8</sup> To achieve this challenge, many efforts have been made to design and prepare highly effective water oxidation catalysts (WOCs) with high turnover frequency (TOF) and low overpotential.<sup>7,9–12</sup> These attempts have led recently to the preparation of WOCs involving various transition metals.<sup>9,13–19</sup> Among these complexes, the monomeric Ru-based complexes have been explored most extensively, due to their structural simplicity, which facilitates elucidation of reaction mechanism and the study of structure activity relationships.<sup>7,9,18,20</sup>

The monomeric Ru-WOCs, differ by their supporting ligands. Despite extensive efforts invested in the development of novel Ru-supporting ligands,<sup>7,19–24</sup> understanding the impact of the ligand on the key O–O bond formation step in  $\text{O}_2$  formation during water oxidation remains scant. For instance, it is not clear what role might be played by the net charge of the ligand and how steric hindrance affects the O–O bond formation. The goal of the present work is to explore the dependence of O–O bond formation reactivity on the structure of the Ru-supporting ligand in typical monomeric Ru-WOCs. Attaining this understanding is key step toward a more complete assessment of the various effects exerted by Ru supporting ligands on the activity of WOCs in their catalytic cycles. The insights gained herein would be helpful and inspiring in future ligand design for developing more

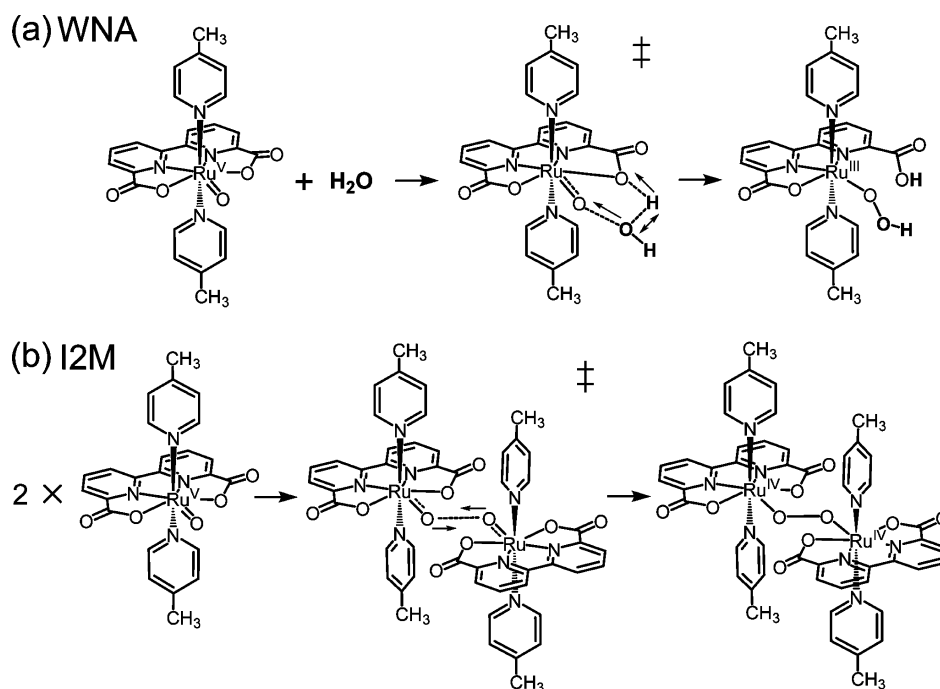
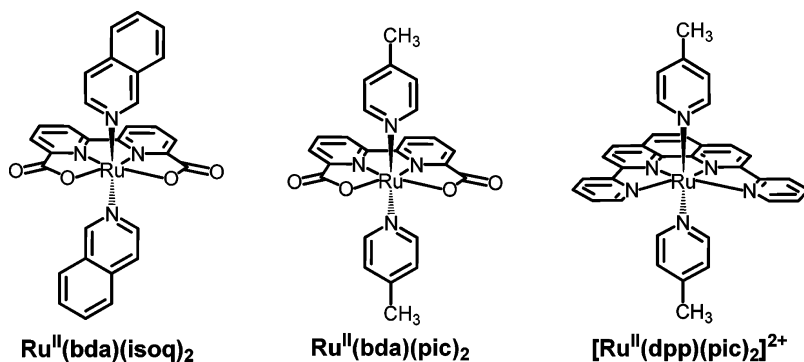
efficient Ru-WOCs. It is also notable that O–O bond formation is not necessarily the rate-limiting step in the water oxidation reactions, despite the fact that sometimes this process was found experimentally to be the most difficult step.<sup>25</sup>

As shown in Scheme 1, there are two widely accepted mechanisms of O–O formation initiated from high-valent  $\text{Ru}^{\text{V}}=\text{O}$  active species. One of these involves a water nucleophilic attack (WNA) on high-valent metal oxo, while the second proceeds via direct coupling of two high-valent metal oxo units (I2M).<sup>11,20–23,26–30</sup> During the WNA mechanism, water attacks as a nucleophile the high-valent metal oxo ( $\text{Ru}^{\text{V}}=\text{O}$ ) moiety of the WOC, as shown in Scheme 1a. This mechanism is also known to transpire during O–O bond formation within OEC in natural photosynthesis.<sup>5,31</sup> Alternatively, in the I2M mechanism in Scheme 1b, O–O bonding occurs between two high-valent metal oxo units ( $\text{Ru}^{\text{V}}=\text{O}$ ). Recent experimental–computational discovery of this I2M mechanism, by Sun, Privalov, Llobet, and their co-workers, in the Ru-based WOCs as  $\text{Ru}^{\text{II}}(\text{bda})(\text{isoq})_2$  in Scheme 2 is a significant progress in the area of Ru-WOCs.<sup>32</sup> However, similar to the situation in the WNA mechanism, here too, in the I2M mechanism, the ligand effect remains largely unexplored.

To explore and identify various ligand effects on the O–O bond formation process during the WNA and I2M mechanisms, we chose experimentally synthesized WOC  $\text{Ru}^{\text{II}}(\text{bda})(\text{pic})_2$  (modeled with **2** in Scheme 3) as a prototype complex,<sup>22</sup> whose O–O formation process including orbital analysis had been explored in both WNA and I2M mechanisms.<sup>23,32</sup> On the

Received: January 2, 2014

Published: June 26, 2014

Scheme 1. Proposed O–O Bond Formation Mechanisms through (a) WNA Pathway and (b) I2M Pathway, Exemplified by WOC  $\text{Ru}^{\text{II}}(\text{bda})(\text{pic})_2$ Scheme 2. Molecular Structures of Some Synthesized Ru-WOCs with Equatorial Tetradentate Ligands<sup>a</sup>

<sup>a</sup>bda = 2,2'-bipyridine-6,6'-dicarboxylate, isoq = isoquinoline, pic = methylpyridine, dpp = 2,9-di(pyrid-2'-yl)-1,10-phenanthroline.

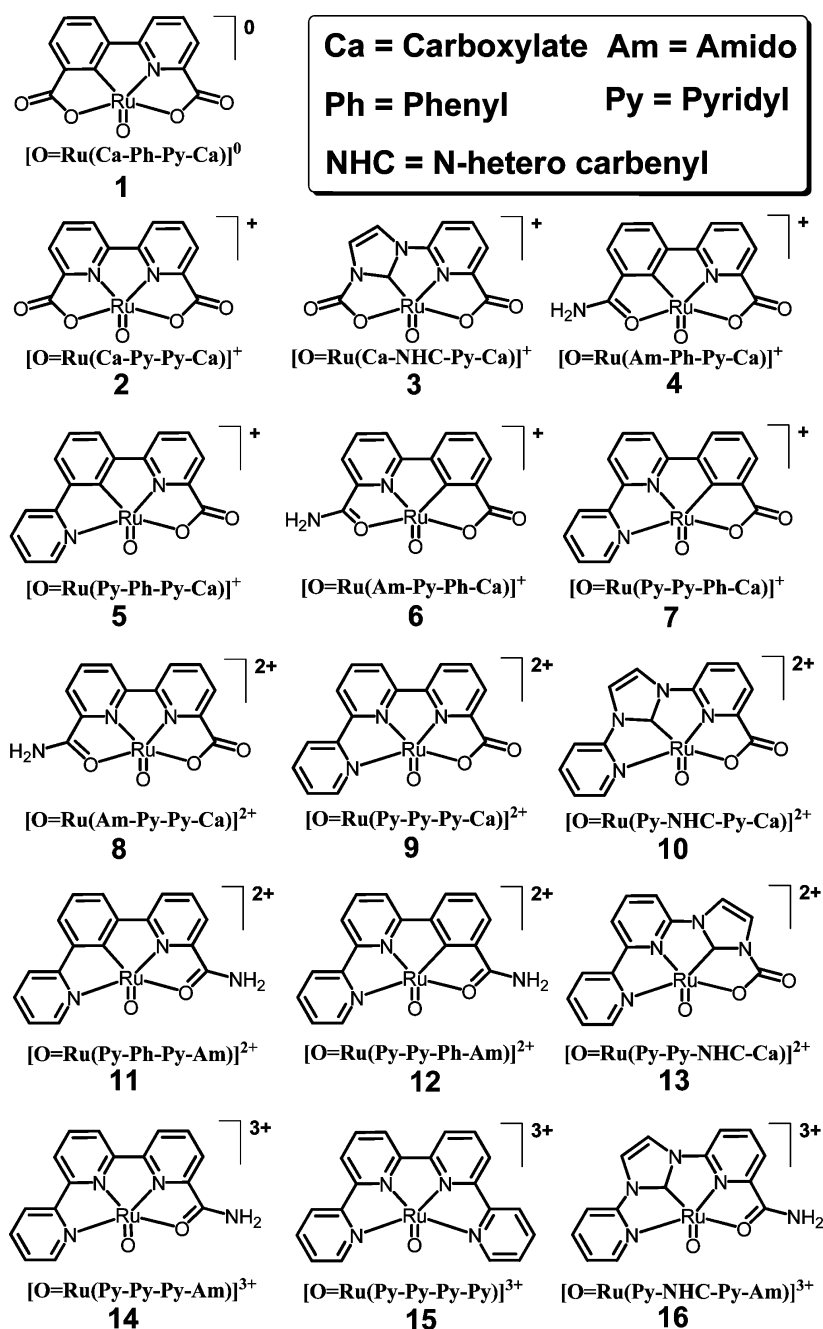
basis of these works for **2** from Sun, Privalov, Llobet, and their co-workers,<sup>22,23,32</sup> by replacement of some ligating groups in its equatorial tetradentate ligand (bda) with pyridyl, phenyl, N-hetero carbenyl (NHC), or amido groups that are commonly used experimentally in ligands for Ru complexes, we systematically designed the series of potential Ru-WOC models in Scheme 3, wherein all the complexes possess high-valent  $\text{Ru}^{\text{V}}=\text{O}$  species as needed in water oxidation. In addition to different equatorial ligands, the charges of these models also vary from 0 to +3. For clarity, we labeled the tetradentate ligands by abbreviating them to the four ligating groups from left to right. In all models, two axial positions are occupied by two pyridine groups, which are not explicitly depicted, but are noted under the structures in Scheme 3. Among these models, **15** is the analogue of  $[\text{Ru}^{\text{II}}(\text{dpp})(\text{pic})_2]^{2+}$  that has been synthesized and applied as an actual WOC in experiment.<sup>33</sup> Different ligands in Scheme 3 may have different net charges, different steric hindrance effects, or different electronic properties. Since, in this work, we are mainly concerned about the barrier difference of various systems with different ligands, except the attacking water in the WNA

mechanism, we did not add more solvent water molecules into the system, which leads to a simpler model than the previous modeling for some specific system.<sup>22,23,32</sup> This work elucidates the roles of all of these factors during the O–O bond formation process by computing and comparing the respective activation barriers. It should be noted that kinetic barriers in this study concern the O–O bond formation between intermediates with the same number of electrons and protons. This feature is different from those electrochemical water oxidation processes with changing numbers of electrons or protons, which had been explored with the approach developed by Nørskov and Rossmeisl et al. in water oxidation on metal and metal-oxide surfaces, and with multinuclear Ru WOCs.<sup>34</sup>

## COMPUTATIONAL DETAILS

All geometries of  $\text{Ru}^{\text{V}}=\text{O}$  species and O–O formation transition states were optimized in water with the PBE0<sup>35</sup> functional using the Ahlrichs' def-SVP and def-SV<sup>36</sup> basis sets on the Ru atom and the other elements. Single-point calculations were performed with both PBE0 and B3LYP<sup>37</sup> functionals using the larger basis set def2-TZVPP<sup>38</sup> (denoted as B2)

Scheme 3. High-Valent Ru<sup>V</sup>=O Active Species in Monomeric Ruthenium WOCs Studied in This Work (Two Pyridine Ligands at Axial Positions Were Omitted for Clarity)



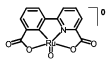
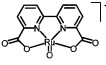
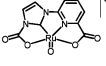
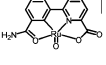
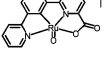
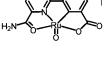
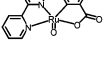
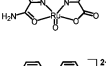
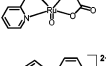
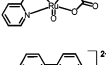
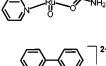
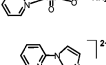
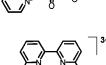
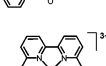
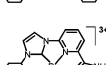
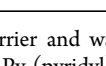
instead. PBE0 and B3LYP had been widely employed in theoretical modeling of O–O bond formation by monomeric Ru-based WOCs.<sup>21–23,25a,32,39–43</sup> Through high-level ab initio coupled cluster calibration study, we have recently shown that PBE0 and B3LYP perform well in barrier calculation of O–O bond formation promoted by Ru<sup>V</sup>=O species with the WNA mechanism.<sup>44</sup> The effect of the water solvent was modeled by the continuum solvation model CPCM,<sup>45</sup> in both single-point and geometry optimization calculations. The harmonic vibrational frequency analysis was used to confirm the transition states (one imaginary frequency) and the Ru<sup>V</sup>=O reactants (no imaginary frequency), as well as to obtain the thermal correction of Gibbs free energy. To compare the barriers more evenly in different systems and mechanisms, we measured the barrier as the energy difference between the transition state and the separated reactants, rather than from the reactant complex. This treatment can avoid the problem of multiple geometric conformations often encountered in the

relatively flexible systems, such as reactant complexes of Ru(V)=O and the attacking H<sub>2</sub>O. Compared with using the reactant complex as the zero point to measure the barrier, this treatment of separated reactants will cause a relatively larger difference between the Gibbs free energy barrier and the electronic energy barrier. However, since the key issue here in this work is often barrier comparison, the difference between these two ways of treating the reactant is minimized. The spin states of a single metal oxo unit in the WNA mechanism (Ru<sup>V</sup>=O) and double metal oxo units in the I2M mechanism were adopted as  $S = 1/2$  (doublet) and  $S = 0$  (singlet), respectively. All calculations were performed with the Gaussian 09 suite of program.<sup>46</sup>

## RESULTS AND DISCUSSION

The energy barriers for O–O bond formation are collected in Table 1 for the WNA and I2M mechanisms of 1–16. Since the

Table 1. Calculated O–O Bond Formation Barriers  $\Delta E^\ddagger$  and  $\Delta G^\ddagger$  (kcal/mol) of All Ru-Based WOCs in Scheme 3 with WNA and I2M Mechanisms<sup>a,b</sup>

Label	Structure	H <sup>+</sup> acceptor <sup>b</sup>	WNA	I2M	WNA	I2M
			$\Delta E^\ddagger$	$\Delta E^\ddagger$	$\Delta G^\ddagger$	$\Delta G^\ddagger$
1		Ca <sub>left</sub>	24.9	11.6	34.8	26.6
		Ca <sub>right</sub>	43.0		53.9	
2		Ca	32.7	10.9	43.8	27.6
3		Ca <sub>left</sub>	16.7	8.6	27.6	23.8
		Ca <sub>right</sub>	39.8		51.0	
4		Ca	36.7	8.7	46.6	26.5
5		Ca	33.7	13.8	44.5	31.1
6		Ca	18.7	6.6	29.0	24.6
7		Ca	25.0	11.6	34.8	27.9
8		Ca	32.7	11.2	43.8	29.4
9		Ca	28.9	15.7	39.2	33.2
		Py	31.5		40.8	
10		Ca	35.6	12.3	47.1	28.8
11		Py	26.5	14.5	35.1	29.9
12		Py	44.8	15.0	55.3	31.6
13		Ca	18.2	14.0	28.4	29.7
14		Py	30.5	21.8	41.3	37.7
15		Py	24.1	46.9	34.7	65.4
16		Py	19.8	17.8	29.9	36.2

<sup>a</sup> $\Delta E^\ddagger$  is the electronic energy barrier and was computed at the PBE0/B2 level in water.  $\Delta G^\ddagger$  is the Gibbs free energy barrier. <sup>b</sup>In the WNA mechanism, Ca (carboxylate) and Py (pyridyl) groups are acting as groups to accept H<sup>+</sup> during O–O bond formation concomitantly coupled with proton transfer. For 1 and 3, as shown in Scheme 3, there are two alternative H<sup>+</sup>-accepting Ca groups with different chemical environments; we use subscript “left” and “right” to distinguish them. Note that “left” corresponds to the Ca group adjacent to Ph or NHC groups.

conclusions of this work remain essentially unchanged from  $\Delta E^\ddagger$  to  $\Delta G^\ddagger$ , below, we only discuss the electronic energy barrier  $\Delta E^\ddagger$ . Inspection of the data reveals that, except for a few cases, which will be discussed later, the I2M barriers are significantly lower than the corresponding WNA barriers. This computed trend is in agreement with the previous DFT calculations for 2 by Privalov et al.<sup>22</sup> However, quantitatively, our WNA barrier for 2 is higher

than the WNA barrier reported before. This difference is mainly due to the larger basis set used in this work (see data in Table S1 in the Supporting Information).

Before we discuss various effects of the Ru supporting ligand on the O–O bond formation barrier, first, we wish to resolve a special issue for the WNA mechanism. As shown in Scheme 1, unlike I2M, in the WNA mechanism, there has to be a proton-

accepting group, which temporarily absorbs the proton released from the water attacking  $\text{Ru}^{\text{V}}=\text{O}$  to form O–O bond formation. The basic side group of the equatorial ligand can play such a role and was explored as a proton-accepting group in previous computational work.<sup>22,23</sup> In some of our WOCs like **9**, there are two different proton-accepting basic groups. To determine which group is apt to accept the proton, we calculated two barriers using the alternative pyridyl (Py) or carboxylate (Ca) groups as proton-accepting groups. The results in Table 1 indicate that Ca confers a lower barrier than Py by 2.6 kcal/mol. Thus, wherever possible, Ca should be used preferentially as proton-accepting groups for the WNA mechanism in the following exploration of various ligand effects on O–O bond formation.

Let us now focus on the WNA barriers in Table 1. For **1**, one can see two significantly different WNA barriers of 24.9 and 43.0 kcal/mol for two side Ca groups as proton-accepting groups. This very large difference of ~20 kcal/mol arises apparently from the Ph group in the ligand in **1**. Concerning the reactant structure of **1**, the  $\text{Ru}-\text{O}_{\text{Ca}}$  bond adjacent to the Ph group is considerably longer than the other one by 0.09 Å. When compared with the corresponding Ph-to-Py substituted ligand in **2** that has a WNA barrier of 32.7 kcal/mol, it is clear that Ph coordination in **1** can substantially lower the O–O formation barrier when the Ph group is in a cis position to the proton-accepting group in the WNA mechanism. In fact, the Ca in the cis position of Ph is more basic. We hereafter call this strong activation “the cis-effect” for the WNA mechanism. On the contrary, the barrier is increased significantly when the Ph group is not at a cis position to the proton-accepting group. In this manner, the Ph group can selectively favor one of the two WNA pathways. It is interesting to see that the carbene group (NHC) in **3** behaves similarly, leading to an even larger barrier difference between cis and non-cis cases (16.7 and 39.8 kcal/mol). Thus, both Ph and NHC exert a cis-effect that lowers the O–O formation barrier in the WNA mechanism.

In the above cases of **1**, **2**, and **3**, two alternative proton-accepting groups are present in one molecule, and one of these is adjacent to a Ph or NHC group. If only one proton-accepting group exists in the complex, the cis-effect is also apparent, such as in the WNA barrier of **6** (18.7 kcal/mol) compared with that of **4** (36.7 kcal/mol), the barrier of **7** (25.0 kcal/mol) compared with that of **5** (33.7 kcal/mol), and the barrier of **13** (18.2 kcal/mol) compared with that of **10** (35.6 kcal/mol).

In addition, the cis-effect is not dependent on the identity of the proton-accepting group. For example, using Py as a proton-accepting group, **16**, which bears an NHC group cis to the proton-accepting group, leads to a barrier of 19.8 kcal/mol, which can be compared with the much higher barrier of 30.5 kcal/mol of **14** having the corresponding NHC-to-Py substituted ligand. Similarly, **11**, which bears a Ph group cis to Py, has a barrier of 26.5 kcal/mol, which is much lower than the barrier of 44.8 kcal/mol for **12**, with the corresponding Ph group being non-cis to Py. The same net charges in the above comparisons also exclude the possibility that such a barrier lowering cis-effect is due to a net charge difference of the high-valent  $\text{Ru}^{\text{V}}=\text{O}$  system. Most likely, the cis group simply confers higher basicity on the corresponding proton-accepting group like Ca that deprotonates water.

Different from WNA, for the I2M mechanism, we only see a tiny shift on the O–O formation barrier by introducing the Ph (11.6 kcal/mol for **1**) or NHC (8.6 kcal/mol for **3**) groups into the ligand to replace Py (10.9 kcal/mol for **2**). In addition, **1**, which bears a net charge of zero, has a slightly higher I2M barrier

than **2** and **3**, which possess net charges of 1+. This result is counterintuitive based on simple Coulomb repulsion between two approaching high-valent  $\text{Ru}^{\text{V}}=\text{O}$  molecules during O–O bond formation in the I2M mechanism, which implies that the net charge of high-valent  $\text{Ru}^{\text{V}}=\text{O}$  species may be screened and may not be a decisive factor for O–O bond formation. This viewpoint can be further supported by the comparison of **8** to **2** (I2M barrier of 11.2 and 10.9 kcal/mol), and of **11** to **5** (I2M barrier of 14.5 and 13.8 kcal/mol). The two tetradentate ligands in each pair share the same coordinating atoms but differ by 1 net charge. The considerable shift due to net charge change can only be seen when the net charge of the WOC becomes even higher, +3, as seen in **14** in comparison with **9** (I2M barriers of 21.8 and 15.7 kcal/mol), and in **16** with **10** (I2M barriers of 17.8 and 12.3 kcal/mol). The shifts of the barrier for these two pairs of WOCs are of similar size, i.e., 6.1 and 5.5 kcal/mol, respectively, with +3 net charge systems bearing a uniformly higher barrier than the +2 ones. This fact is in line with the intuition based on simple physics of Coulomb repulsion. Thus, we can conclude that, only for a very positively charged system such as +3, the Coulomb repulsion begins to significantly affect the I2M O–O bond formation barrier, the magnitude of which is almost independent of the specifics of ligands. Having examined the net charge effect on the I2M O–O formation barrier, a question arises: Is there a charge effect also in the WNA mechanism? Since the mechanism involves nucleophilic attack, it is natural to expect that positive net charges will generally favor this mechanism due to enhanced electrophilicity of the  $\text{Ru}^{\text{V}}=\text{O}$  complex. To clarify this issue, we can compare the WNA barrier of **6** (18.7 kcal/mol) with the corresponding one of **1** (24.9 kcal/mol,  $\text{Ca}_{\text{left}}$  as proton-accepting group), which exhibits a shift of 6.2 kcal/mol. Because **1** relates to **6** by replacement of one side carboxylate with an amido group, while sharing the exact same coordinating atoms, we can thus unambiguously assign this shift to the net charge effect. Interestingly, if we compare the WNA barrier of **4** (36.7 kcal/mol), which does not have a cis-effect like in **6**, with the corresponding one of **1** (43.0 kcal/mol,  $\text{Ca}_{\text{right}}$  as proton-accepting group), we see a shift of 6.3 kcal/mol for the net charge effect. The nearly identical shifts for **4** and **6** indicate that the net charge is independent of the cis-effect, which should be the case if we really reveal here a new ligand factor for the O–O bond formation barrier.

This net charge effect is approximately transferable. To clearly see this, we can perform a Ph-to-NHC replacement in the ligand, without changing the coordinating atoms while increasing the net charge of the WOC by 1. Applying this replacement for **1/11/7**, we get the corresponding NHC group-containing systems **3/16/13**, and we find that the net charge shifts of the WNA barriers are 8.2/6.7/6.8 kcal/mol, respectively (WNA barriers of 24.9/26.5/25.0 kcal/mol for **1/11/7** and 16.7/19.8/18.2 kcal/mol for **3/16/13**). Note that these species include all possible net charges under study, i.e., 0, +1, +2, and +3, which means that, unlike in the I2M mechanism, the existence and magnitude of the net charge effect in the WNA mechanism are independent of the specific charges of the system.

The net charges increasing can lead to the barrier decreasing for the WNA mechanism and the barrier increasing for the I2M barriers. In addition, the cis-effect would lead to lowering of the WNA barriers. As a result, for the complexes **13** and **16**, we find that the differences between WNA barriers and I2M barriers are only 4.2 and 2.0 kcal/mol, respectively. These values are quite small, which implies that the water oxidation mechanism could switch from I2M to WNA if the errors of barrier predictions of

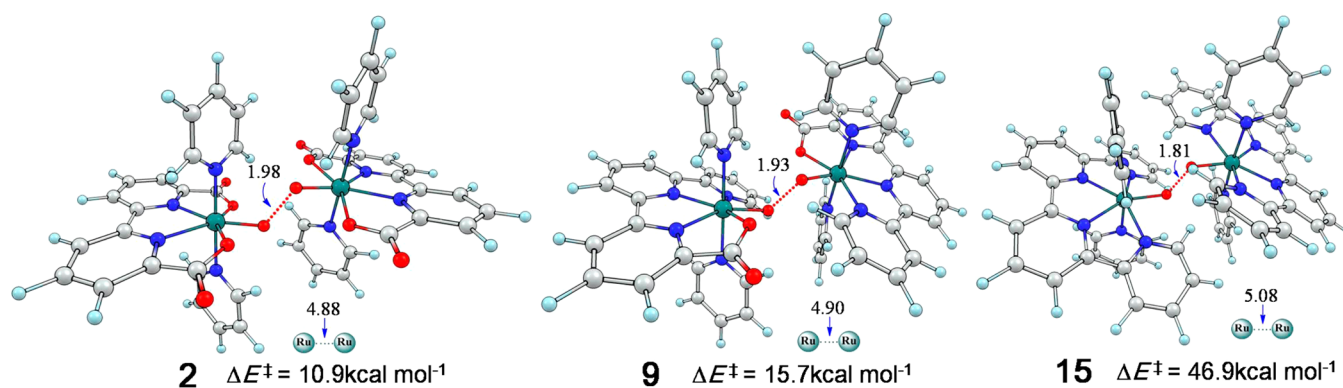


**Figure 1.** Transition-state structures of O–O bond formation catalyzed with **2**, **9**, and **15** following the I2M mechanism.

these two mechanisms are similar. It is interesting to see that a recent work by experimentalists has showed that subtle ligand modifications for a Ru WOC can cause a change in the O–O bond formation mechanism due to close I2M and WNA barriers.<sup>47</sup>

Finally, for the I2M mechanism, except for the net charge effect already discussed above, we identified another effect, which plays an important role in some specific system. **2**, **9**, and **15** constitute a series of complexes generated from one another by successive replacement of two side Ca groups by Py in the tetradentate equatorial ligand of **2**. Comparing their respective I2M barriers, one can find that, from **2** to **9**, the I2M barrier only changes moderately by 4.8 kcal/mol (from 10.9 to 15.7 kcal/mol), but from **9** to **15**, there is a huge increase of 31.2 kcal/mol. What is the reason for such a huge change leading to the highest energy barrier of all? Above, we have shown that the net charge effect from +2 to +3 can only account for a very limited increase of the I2M barrier, by around 5 kcal/mol. Hence, this huge barrier increase cannot be interpreted by changes in net charges; it originates in a steric effect. As shown in Figure 1, for the I2M transition-state (TS) structure with complex **2**, the tetradentate equatorial ligands of two oxo metal moieties show hardly any distortion and keep in a plane, with the two axial pyridyl ligands being parallel to each other. These indicate almost no steric repulsion between the two oxo metal moieties in the TS. Although **9** has a larger tetradentate ligands, it has only one more side pyridyl ligand than **2**, and hence, the two metal oxo units adopt a head-to-tail (Ca-to-Py) relationship between the two tetradentate ligands and thereby avoid strong steric repulsion in O–O bond forming TS. In contrast, two crowded tetradentate ligands with two side pyridyl groups prevent complex **15** to assume a head-to-tail pattern contact and lead to a much higher barrier in O–O bond formation. From Figure 1, the O–O bond lengths of the three TS structures for O–O bond formation are 1.98 Å (**2**), 1.93 Å (**9**), and 1.81 Å (**15**), respectively, which indicate that TS is becoming increasingly late in character on going from **2** through **9** to **15**, in line with steric hindrance disfavoring the O–O bond formation. In addition, their corresponding Ru–Ru distances are in reversed order of 4.88 Å (**2**), 4.90 Å (**9**), and 5.08 Å (**15**), which means that the Ru center is separated away along this series. This can also be accounted for by the steric repulsion between the ligands of two Ru centers because it is the contact of the Ru-surrounding ligands that determines the Ru–Ru distance. A longer Ru–Ru distance corresponds to larger steric hindrance between two high-valent Ru<sup>V</sup>=O fragments. Excluding this exceptional case of **15** with a very crowded ligand environment, the barrier in the I2M

mechanism is generally less affected by ligand variation than the barrier in the WNA mechanism, which implies that the space left for reactivity adjustment by the ligand in the I2M mechanism is not as large as that in the WNA mechanism.

## CONCLUSIONS

In summary, several effects exerted by the tetradentate Ru-supporting ligand on the activation barrier of O–O bond formation in the water oxidation process following both WNA and I2M mechanisms are revealed in this work. We found that (1) the phenyl or carbene group in the tetradentate Ru-supporting ligand can facilitate the WNA O–O bond formation compared with a pyridyl group. Phenyl and carbene groups exert a selective participation of the *cis*-proton-accepting moiety in the WNA O–O formation mode. (2) In line with the chemical intuition, the net charge of the system is found to have some uniform shifting effect on O–O bond formation for the WNA mechanism, with lowering of the WNA barrier by a more positively charged system. For the I2M mechanism, however, the simple intuition about Coulomb repulsion effects on the barriers manifests only when the charge reaches a high value of +3. (3) For a very bulky ligand, steric hindrance can severely increase the barrier in the I2M mechanism. All of these findings are useful and inspiring in the future ligand design for monomeric Ru-based WOCs in searching for a highly effective O–O formation process to increase the overall performance of WOCs.

## ASSOCIATED CONTENT

### Supporting Information

Two tables of computational results, and Cartesian coordinates. This material is available free of charge via the Internet at <http://pubs.acs.org>.

## AUTHOR INFORMATION

### Corresponding Authors

\*E-mail: [chenh@iccas.ac.cn](mailto:chenh@iccas.ac.cn) (H.C.).

\*E-mail: [jnyao@iccas.ac.cn](mailto:jnyao@iccas.ac.cn) (J.Y.).

### Notes

The authors declare no competing financial interest.

## ACKNOWLEDGMENTS

This work is supported by the National Natural Science Foundation of China (Nos. 21290194, 21221002), the National Basic Research Program of China (No. 2011CB808402), and the Chinese Academy of Sciences. The research of S.S. is supported by an ISF grant (ISF 1183/13).

## REFERENCES

- (1) Sun, L. C.; Hammarstrom, L.; Åkermark, B.; Styring, S. *Chem. Soc. Rev.* **2001**, *30*, 36–49.
- (2) Meyer, T. J. *Acc. Chem. Res.* **1989**, *22*, 163–170.
- (3) Rüttinger, W.; Dismukes, G. C. *Chem. Rev.* **1997**, *97*, 1–24.
- (4) Bard, A. J.; Fox, M. A. *Acc. Chem. Res.* **1995**, *28*, 141–145.
- (5) Yagi, M.; Kaneko, M. *Chem. Rev.* **2001**, *101*, 21–35.
- (6) McEvoy, J. P.; Brudvig, G. W. *Chem. Rev.* **2006**, *106*, 4455–4483.
- (7) Hetterscheid, D. G. H.; Reek, J. N. H. *Angew. Chem., Int. Ed.* **2012**, *51*, 9740–9747.
- (8) Umena, Y.; Kawakami, K.; Shen, J.-R.; Kamiya, N. *Nature* **2011**, *473*, 55–60.
- (9) Cao, R.; Lai, W. Z.; Du, P. W. *Energy Environ. Sci.* **2012**, *5*, 8134–8157.
- (10) Jiang, Y.; Li, F.; Zhang, B. B.; Li, X. N.; Wang, X. H.; Huang, F.; Sun, L. C. *Angew. Chem., Int. Ed.* **2013**, *52*, 3398–3401.
- (11) An, J. X.; Duan, L. L.; Sun, L. C. *Faraday Discuss.* **2012**, *155*, 267–275.
- (12) Artero, V.; Chavarot-Kerlidou, M.; Fontecave, M. *Angew. Chem., Int. Ed.* **2011**, *50*, 7238–7266.
- (13) Barnett, S. M.; Goldberg, K. I.; Mayer, J. M. *Nat. Chem.* **2012**, *4*, 498–502.
- (14) (a) Ellis, W. C.; McDaniel, N. D.; Bernhard, S.; Collins, T. J. *J. Am. Chem. Soc.* **2010**, *132*, 10990–10991. (b) Fillol, J. L.; Codolà, Z.; Garcia-Bosch, I.; Gómez, L.; Pla, J. J.; Costas, M. *Nat. Chem.* **2011**, *3*, 807–813. (c) Chen, G.; Chen, L. J.; Ng, S.-M.; Man, W.-L.; Lau, T.-C. *Angew. Chem., Int. Ed.* **2013**, *52*, 1789–1791.
- (15) (a) Kanan, M. W.; Nocera, D. G. *Science* **2008**, *321*, 1072–1075. (b) Shevchenko, D.; Anderlund, M. F.; Thapper, A.; Styring, S. *Energy Environ. Sci.* **2011**, *4*, 1284–1287. (c) Yin, Q. S.; Tan, J. M.; Besson, C.; Geletii, Y. V.; Musaev, D. G.; Kuznetsov, A. E.; Luo, Z.; Hardcastle, K. I.; Hill, C. L. *Science* **2010**, *328*, 342–345.
- (16) Dismukes, G. C.; Brimblecombe, R.; Felton, G. A. N.; Pryadun, R. S.; Sheats, J. E.; Spiccia, L.; Swiegers, G. F. *Acc. Chem. Res.* **2009**, *42*, 1935–1943.
- (17) Dincă, M.; Surendranath, Y.; Nocera, D. G. *Proc. Natl. Acad. Sci. U.S.A.* **2010**, *107*, 10337–10341.
- (18) Wasylenko, D. J.; Palmer, R. D.; Berlinguette, C. P. *Chem. Commun.* **2013**, *49*, 218–227.
- (19) Dau, H.; Limberg, C.; Reier, T.; Risch, M.; Roggan, S.; Strasser, P. *ChemCatChem* **2010**, *2*, 724–761.
- (20) Zhang, G. L.; Chen, K. J.; Chen, H.; Yao, J. N.; Shaik, S. *Inorg. Chem.* **2013**, *52*, 5088–5096.
- (21) Nyhlén, J.; Duan, L. L.; Åkermark, B.; Sun, L. C.; Privalov, T. *Angew. Chem., Int. Ed.* **2010**, *49*, 1773–1777.
- (22) Tong, L. P.; Duan, L. L.; Xu, Y. H.; Privalov, T.; Sun, L. C. *Angew. Chem., Int. Ed.* **2011**, *50*, 445–449.
- (23) Privalov, T.; Åkermark, B.; Sun, L. C. *Chem.—Eur. J.* **2011**, *17*, 8313–8317.
- (24) Tseng, H.-W.; Zong, R. F.; Muckerman, J. T.; Thummel, R. *Inorg. Chem.* **2008**, *47*, 11763–11773.
- (25) (a) Lin, X. S.; Hu, X. Q.; Concepcion, J. J.; Chen, Z. F.; Liu, S. B.; Meyer, T. J.; Yang, W. T. *Proc. Natl. Acad. Sci. U.S.A.* **2012**, *109*, 15669–15672. (b) Concepcion, J. J.; Jurss, J. W.; Norris, M. R.; Chen, Z. F.; Templeton, J. L.; Meyer, T. J. *Inorg. Chem.* **2010**, *49*, 1277–1279. (c) Concepcion, J. J.; Tsai, M.-K.; Muckerman, J. T.; Meyer, T. J. *J. Am. Chem. Soc.* **2010**, *132*, 1545–1557. (d) Concepcion, J. J.; Jurss, J. W.; Templeton, J. L.; Meyer, T. J. *J. Am. Chem. Soc.* **2008**, *130*, 16462–16463. (e) Wasylenko, D. J.; Ganesamoorthy, C.; Henderson, M. A.; Koivisto, B. D.; Osthoff, H. D.; Berlinguette, C. P. *J. Am. Chem. Soc.* **2010**, *132*, 16094–16106.
- (26) Romain, S.; Vigara, L.; Llobet, A. *Acc. Chem. Res.* **2009**, *42*, 1944–1953.
- (27) Duan, L. L.; Fischer, A.; Xu, Y. H.; Sun, L. C. *J. Am. Chem. Soc.* **2009**, *131*, 10397–10399.
- (28) Bozoglian, F.; Romain, S.; Erten, M. Z.; Todorova, T. K.; Sens, C.; Mola, J.; Rodríguez, M.; Romero, I.; Benet-Buchholz, J.; Fontrodona, X.; Cramer, C. J.; Gagliardi, L.; Llobet, A. *J. Am. Chem. Soc.* **2009**, *131*, 15176–15187.
- (29) Vigara, L.; Ertem, M. Z.; Planas, N.; Bozoglian, F.; Leidel, N.; Dau, H.; Haumann, M.; Gagliardi, L.; Cramer, C. J.; Llobet, A. *Chem. Sci.* **2012**, *3*, 2576–2586.
- (30) Poater, A. *Catal. Commun.* **2014**, *44*, 2–5.
- (31) There is also a viewpoint that O–O bond formation in OEC is via an oxo coupling mechanism; see: Siegbahn, P. E. M. *Biochim. Biophys. Acta, Bioenerg.* **2013**, *1827*, 1003–1019.
- (32) Duan, L. L.; Bozoglian, F.; Mandal, S.; Stewart, B.; Privalov, T.; Llobet, A.; Sun, L. C. *Nat. Chem.* **2012**, *4*, 418–423.
- (33) Zhang, G.; Zong, R. F.; Tseng, H.-W.; Thummel, R. P. *Inorg. Chem.* **2008**, *47*, 990–998.
- (34) (a) Rossmeis, J.; Logadottir, A.; Nørskov, J. K. *Chem. Phys.* **2005**, *319*, 178–184. (b) Rossmeis, J.; Nørskov, J. K.; Taylor, C. D.; Janik, M. J.; Neurock, M. *J. Phys. Chem. B* **2006**, *110*, 21833–21839. (c) Piccinin, S.; Sartorel, A.; Aquilanti, G.; Goldoni, A.; Bonchio, M.; Fabris, S. *Proc. Natl. Acad. Sci. U.S.A.* **2013**, *110*, 4917–4922.
- (35) (a) Perdew, J. P.; Burke, K.; Ernzerhof, M. *Phys. Rev. Lett.* **1996**, *77*, 3865–3868. (b) Ernzerhof, M.; Scuseria, G. E. *J. Chem. Phys.* **1999**, *110*, 5029–5036. (c) Adamo, C.; Barone, V. *J. Chem. Phys.* **1999**, *110*, 6158–6170.
- (36) Schäfer, A.; Horn, H.; Ahlrichs, R. *J. Chem. Phys.* **1992**, *97*, 2571–2577.
- (37) (a) Becke, A. D. *Phys. Rev. A* **1988**, *38*, 3098–3100. (b) Lee, C. T.; Yang, W. T.; Parr, R. G. *Phys. Rev. B* **1988**, *37*, 785–789. (c) Becke, A. D. *J. Chem. Phys.* **1993**, *98*, 5648–5652.
- (38) Weigend, F.; Ahlrichs, R. *Phys. Chem. Chem. Phys.* **2005**, *7*, 3297–3305.
- (39) Lai, W. Z.; Cao, R.; Dong, G.; Shaik, S.; Yao, J. N.; Chen, H. *J. Phys. Chem. Lett.* **2012**, *3*, 2315–2319.
- (40) Chen, Z. F.; Concepcion, J. J.; Hu, X. Q.; Yang, W. T.; Hoertz, P. G.; Meyer, T. J. *Proc. Natl. Acad. Sci. U.S.A.* **2010**, *107*, 7225–7229.
- (41) Wang, L.-P.; Wu, Q.; Voorhis, T. V. *Inorg. Chem.* **2010**, *49*, 4543–4553.
- (42) Hughes, T. F.; Friesner, R. A. *J. Phys. Chem. B* **2011**, *115*, 9280–9289.
- (43) Lang, Z.-L.; Yang, G.-C.; Ma, N.-N.; Wen, S.-Z.; Yan, L.-K.; Guan, W.; Su, Z.-M. *Dalton Trans.* **2013**, *42*, 10617–10625.
- (44) Kang, R. H.; Yao, J. N.; Chen, H. *J. Chem. Theory Comput.* **2013**, *9*, 1872–1879.
- (45) (a) Barone, V.; Cossi, M. *J. Phys. Chem. A* **1998**, *102*, 1995–2001. (b) Cossi, M.; Rega, N.; Scalmani, G.; Barone, V. *J. Comput. Chem.* **2003**, *24*, 669–681.
- (46) Frisch, M. J.; Trucks, G. W.; Schlegel, H. B.; Scuseria, G. E.; Robb, M. A.; Cheeseman, J. R.; Scalmani, G.; Barone, V.; Mennucci, B.; Petersson, G. A.; Nakatsuji, H.; Caricato, M.; Li, X.; Hratchian, H. P.; Izmaylov, A. F.; Bloino, J.; Zheng, G.; Sonnenberg, J. L.; Hada, M.; Ehara, M.; Toyota, K.; Fukuda, R.; Hasegawa, J.; Ishida, M.; Nakajima, T.; Honda, Y.; Kitao, O.; Nakai, H.; Vreven, T.; Montgomery, J. A., Jr.; Peralta, J. E.; Ogliaro, F.; Bearpark, M.; Heyd, J. J.; Brothers, E.; Kudin, K. N.; Staroverov, V. N.; Kobayashi, R.; Normand, J.; Raghavachari, K.; Rendell, A.; Burant, J. C.; Iyengar, S. S.; Tomasi, J.; Cossi, M.; Rega, N.; Millam, J. M.; Klene, M.; Knox, J. E.; Cross, J. B.; Bakken, V.; Adamo, C.; Jaramillo, J.; Gomperts, R.; Stratmann, R. E.; Yazyev, O.; Austin, A. J.; Cammi, R.; Pomelli, C.; Ochterski, J. W.; Martin, R. L.; Morokuma, K.; Zakrzewski, V. G.; Voth, G. A.; Salvador, P.; Dannenberg, J. J.; Dapprich, S.; Daniels, A. D.; Farkas, O.; Foresman, J. B.; Ortiz, J. V.; Cioslowski, J.; Fox, D. J. *Gaussian 09*, revision C.01; Gaussian, Inc.: Wallingford, CT, 2009.
- (47) Neudeck, S.; Maji, S.; López, I.; Meyer, S.; Meyer, F.; Llobet, A. *J. Am. Chem. Soc.* **2014**, *136*, 24–27.